Green Chemistry

PAPER

View Article Online
View Journal | View Issue

Cite this: *Green Chem.*, 2014, **16**, 3230

Boronate microparticle-supported nano-palladium and nano-gold catalysts for chemoselective hydrogenation of cinnamaldehyde in environmentally preferable solvents†

Seika Fujiwara,[a] Naoto Takanashi,[a] Ryuhei Nishiyabu[a] and Yuji Kubo*[a,b]

Received 4th March 2014,
Accepted 12th April 2014

DOI: 10.1039/c4gc00383g

www.rsc.org/greenchem

Dispersible self-assembled boronate polymers can serve as support materials for metal nanoparticle catalysts. As a proof-of-concept, catalytic systems for the chemoselective hydrogenation of cinnamaldehyde (**CA**) were prepared by the $NaBH_4$ reduction of $PdCl_4^{2-}$ and $AuCl_4^-$ in methanol, in the presence of polyethyleneimine (PEI)-coated boronate particles (**BPs**) composed of polymeric 3-benzo-2,4,8,10-tetraoxa-3,9-diboraspiro[5.5]undecane. The Pd-deposited **BP** (**Pd/BP**) showed highly selective catalytic activity for the hydrogenation of **CA** to hydrocinnamaldehyde (**HCA**) under 0.1 MPa of H_2 at 25 °C in environmentally preferable solvents such as water and methanol. Of particular note is the recyclability of the hydrogenation catalyst in methanol; repeated 4 h reactions afforded **HCA** in >90% selectivity with a reaction conversion of 100%. On another front, when the corresponding Au catalyst (**Au/BP**) was used in the hydrogenation in water, a favorable selective reduction of C═O to cinnamyl alcohol (**CAL**) (selectivity ≈ 80%) was obtained with 78% reaction conversion under 0.8 MPa of H_2 at 80 °C for 12 h. The potential use of **BP**-supported metal nanoparticles as green catalysts is discussed.

Introduction

There has been growing interest in various fields of materials science in developing highly ordered self-assemblies of molecular modules into larger supramolecular entities with well-defined morphologies.[1] Such an approach is advantageous in providing support materials for heterogeneous catalysts; to date, polymeric nanotubes,[2] microporous polymers,[3] globular-aggregates,[4] and polymeric nanofibers,[5] as well as metal–organic frameworks[6] and covalent organic frameworks,[7] have been reported. The use of phenylboronic acid complexation with diols and their congeners[8] is an alternative way to construct well-defined supramolecular aggregates.[9] Indeed, sequential boronate esterification of benzene-1,4-diboronic acid with pentaerythritol produced mono-dispersed flower-like support materials (**BP**) where gold nanoparticles (Au NPs) could be developed to provide heterogeneous catalysts for the reduction of nitroaromatic compounds.[10] During this work, we found that **BP** forms a stable dispersion in water,[11] which motivated us to apply **BP**-supported metal nanoparticles as catalysts for sustainable chemical synthesis.[12] Because of environmental concerns, reactions in non-flammable and environmentally friendly solvents such as water at room temperature are desirable. In addition, simple alcohols such as methanol and ethanol are environmentally preferable solvents[13] that are water-soluble, biodegradable, and occur naturally in the environment.

With this in mind, our attention has been focused on selective hydrogenation reactions of α,β-unsaturated aldehydes, which have been widely investigated in catalyst chemistry.[14] Among them, cinnamaldehyde (**CA**), being composed of vinyl (C═C) and carbonyl (C═O) groups, is an important substrate for hydrogenation because the reduction of the vinyl segment gives hydrocinnamaldehyde (**HCA**), which is a key intermediate in the preparation of pharmaceuticals.[15] Cinnamyl alcohol (**CAL**) is produced through hydrogenation of the carbonyl groups and is widely used in perfumery and as a deodorant.[16] Further hydrogenation leads to the production of 3-phenylpropanol (**PPL**). As such, the selective synthesis of both **HCA** and **CAL** is highly desired in fine chemical synthesis. To date, a number of transition metal-catalyzed hydrogenation methods have been applied to this end in chemoselective reactions.[17,18] Pd NP-based catalysts are one of the most promising systems for selective hydrogenation of the C═C bond; however, there are few reports on Pd catalysts that are applicable to green

---

[a] *Department of Applied Chemistry, Graduate School of Urban Environmental Sciences, Tokyo Metropolitan University, 1-1 Minami-ohsawa, Hachioji, Tokyo 192-0397, Japan. E-mail: yujik@tmu.ac.jp; Fax: +81 42-677-3134; Tel: +81 42-677-3134*
[b] *Research Center for Gold Chemistry, Tokyo Metropolitan University, Japan*

† Electronic supplementary information (ESI) available: Experimental data (Fig. S1–S10). See DOI: 10.1039/c4gc00383g

solvent processes in which comparatively larger amounts of catalysts[19] or higher pressures of H_2[20] are required. In addition, regarding the selective hydrogenation to **CAL** in water,[21] the use of polymer-supported Au NPs as catalysts remains challenging.

Herein, we describe well-defined boronate self-assemblies (**BPs**) with Pd or Au NPs on their surface and characterize the **BPs** using spectroscopic and electron microscopic data. It is interesting to note that Pd NPs with an average diameter of 1.52 ± 0.44 nm were evenly deposited on the surface, so that the Pd-deposited **BP** (**Pd**/**BP**) exhibited an excellent catalytic activity for the hydrogenation of **CA** to **HCA** with a high selectivity under 0.1 MPa of H_2 at 25 °C in environmentally preferable solvents such as water and MeOH. Its reusability for the hydrogenation in MeOH was also investigated. On the other hand, **BP**-supported Au NPs (**Au**/**BP**) showed a fair activity for selective hydrogenation to **CAL** under 0.8 MPa of H_2 at 80 °C in water. We highlight that boronate self-assemblies are advantageous as support materials for preparation of green catalysts.

Experimental section

Materials

Sodium borohydride ($NaBH_4$) and methanol were used as received. Tetrahydrofuran, anisole and cinnamaldehyde (**CA**) were distilled before use. Palladium(II) chloride ($PdCl_2$), hydrogen tetrachloroaurate(III) tetrahydrate ($HAuCl_4 \cdot 4H_2O$), and linear polyethyleneimine (MW: 25000) were purchased from Wako, Kanto Chemical, and Polymersciences, respectively. Boronate microparticles (**BPs**) composed of polymeric 3-benzo-2,4,8,10-tetraoxa-3,9-diboraspiro[5.5]-undecane were prepared from benzene-1,4-diboronic acid and pentaerythritol according to previously reported procedures (Fig. 1),[10] and their averaged diameters were 1.6 ± 0.3 μm (Fig. S1 in the ESI†). PEI-coated SiO_2, being used as a support material of a control catalyst, was purchased from Aldrich (246743-10ML).

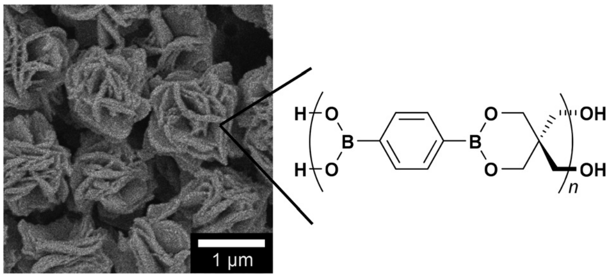

Fig. 1 FE-SEM image of boronate particles (**BPs**).

Characterization

Field-emission scanning electron microscopy (FE-SEM) was performed using a JEOL JSM-7500F (acceleration voltage of 5 kV). Transmission electron microscopy (TEM) was performed using a JEOL JEM-3200FS (acceleration voltage, 300 kV). For FE-SEM measurements, **BPs** collected on a polycarbonate type membrane filter (pore size, 0.2 μm (GRADE: K020A047A), Advantec Ltd) by filtration were employed. The sample was coated with Au on an EIKO IB3 ion coater. TEM measurement was conducted as follows: a suspension of **Pd**/**BP** or **Au**/**BP** was put on a micro grid (Cu200mesh, JEOL Ltd) and the excess solution was immediately absorbed using a filtration paper. The resulting grid was dried in a vacuum and measured without staining. Solid-state ^{13}C cross-polarization-magic angle spinning (CP-MAS) NMR was measured by a JEOL ECA 400SS spectrometer. The observation frequency was 100.53 MHz for ^{13}C. The spectrometer is equipped with a 3.2 mm MAS probehead capable of producing an MAS speed of 18 kHz. Spectra were obtained using a ^{1}H–^{13}C CP with a contact time of 2 ms, an acquisition time of 25.5 ms, a recycle delay of 5 s between scans, and an MAS speed of 18 kHz. The ^{13}C chemical shifts were calibrated using adamantine (δ = 29.5 ppm) as an external standard relative to tetramethylsilane (TMS; δ = 0 ppm). The ^{11}B dipolar decoupling (DD)-MAS NMR spectrum was also measured using boric acid (H_3BO_3) saturated aqueous solution (δ = 19.49 ppm) as an external standard relative to boron trifluoride etherate ($BF_3 \cdot O(C_2H_5)_2$; δ = 0 ppm). Powder X-ray diffraction (PXRD) data were collected by a Rigaku RINT-TTR III X-ray diffractometer with Cu Kα radiation. Thermal gravimetric analysis (TGA) was conducted using a SHIMADZU DTG-60H with a scan rate of 5 °C min^{-1} and a scan range from 24.1 to 865.7 °C under a N_2 flow (50 mL min^{-1}) where an alumina pan was used. Zeta potential measurements for **BP** and polyethyleneimine (PEI)-coated **BP** in methanol (1 g L^{-1}) were performed using an ELSZ-2 (OTSUKA ELECTRONICS) instrument. Atomic absorption spectroscopy for determination of the amount of metal (Pd or Au) deposited on the corresponding hybrids was performed using a SHIMADZU AA-6200. The X-ray photoelectron spectrum (XPS) was acquired using a JPS-9010MX instrument where Mg Kα radiation ($h\nu$ = 1253.6 eV) was employed. For preparation of sample solutions, **BP**-supported metal nanoparticles were added to aqua regia and the mixture was allowed to stand for 12 h to complete the digestion of palladium and gold. The specific surface area was calculated by the BET (Brunauer–Emmett–Teller) method using Micrometer Trister 3000. Identification and quantitative analysis of the products for catalytic tests were performed using a SHIMADZU GC-2010 equipped with an Agilent Technologies 7890A (GC) with an HP-5 capillary column (0.32 mm i.d., 30 m), respectively.

Preparation of boronate-supported metal nanoparticles

To a dispersion solution of **BPs** (1.4 g, 6.09×10^{-3} mol $unit^{-1}$)[22] in MeOH was added polyethyleneimine (PEI) (525 mg, 1.22×10^{-2} mol $unit^{-1}$)[22] at room temperature. The mixture was sonicated for 5 min using an ultrasonic bath and was then allowed to stand for 25 min at room temperature. Filtration and drying under vacuum afforded PEI-coated **BP** as a white solid (1.33 g). The procedure for the preparation of **Pd**/**BP** is as follows: PEI-coated **BP** (600 mg) was dispersed in 0.1 N HCl (295 mL), and 0.1 N HCl solution of $PdCl_2$ (4.68 mL, 2.41×10^{-2} M) was then added to the solution. The resulting mixture was sonicated for 5 min using an ultrasonic bath. After being allowed to stand for 25 min, the produced solids were collected by filtration and were then dispersed in MeOH (300 mL) using an ultrasonic bath. Subsequent addition of $NaBH_4$ (203 mg) into the solution, sonication for 5 min, aging for 25 min, and washing with MeOH afforded **Pd/BP** (497 mg) as a gray solid, the amount of loaded Pd being 0.66 wt%. As a comparison, SiO_2-supported Pd nanoparticles **Pd/SiO$_2$** were prepared in a similar way by stirring $PdCl_2$ (2.34 mL, 2.41×10^{-2} M) in 0.1 N HCl in the presence of PEI-coated SiO_2 (Aldrich, 300 mg), followed by adding $NaBH_4$ (106 mg) to produce **Pd/SiO$_2$** as a dark brown solid (264.1 mg), the amount of loaded Pd being 1.40 wt%.

For preparing **Au/BP**, the procedure is as follows: PEI-coated **BP** (640 mg) was dispersed in MeOH (317 mL), and $HAuCl_4 \cdot 4H_2O$ (26.8 mg) dissolved in 3.5 mL MeOH was added to the solution. The resulting mixture was sonicated for 5 min using an ultrasonic bath. After being allowed to stand for 25 min at room temperature, the resulting solid was collected by filtration and was then dispersed in MeOH (320 mL) using an ultrasonic bath. Subsequent addition of $NaBH_4$ (268 mg) into the solution, sonication for 5 min, aging for 25 min, and washing with MeOH afforded **Au/BP** as a violet solid (538 mg), the amount of loaded Au being 2.1 wt%.

General procedure for the hydrogenation of CA over Pd/BP or Pd/SiO$_2$

Dispersed solution (3 mL) involving **CA** (39.6 mg, 0.3 mmol) and **Pd/BP** (24.4 mg, Pd: 0.5 mol%) was placed in a stainless steel autoclave. After adding a magnetic stirring bar into the solution, hydrogen was then introduced into the autoclave. The mixture was stirred under 0.1 MPa of H_2 at 25 °C. After the reduction, the reaction mixture was extracted with an organic solvent, filtered, and analyzed by GC using anisole as an internal standard. A control experiment using **Pd/SiO$_2$** (11.9 mg, Pd: 0.5 mol%) was performed under similar conditions.

General procedure for the hydrogenation of CA over Au/BP

Au/BP (32.8 mg; Au 1.1 mol%), **CA** (39.6 mg, 0.3 mmol), H_2O (3 mL), and a magnetic stirring bar were placed in a stainless steel autoclave. Hydrogen was then introduced into the autoclave, and the mixture was stirred under 0.8 MPa of H_2 at 80 °C. After the reaction, hydrogen was removed and the reaction mixture was extracted with tetrahydrofuran, filtered, and analyzed by GC using anisole as an internal standard.

Results and discussion

Preparation of boronate-supported metal nanoparticles

The boronate support material **BP** was easily prepared according to a previously reported procedure.[10] Briefly, a solution of benzene-1,4-diboronic acid and pentaerythritol was aged in THF at room temperature for 48 h. Monodispersed flower-like microparticles were obtained with an average diameter of 1.6 ± 0.3 μm (Fig. S1 in the ESI†). Assignment of the building units of the microparticles was conducted using ^{13}C CPMAS NMR and ^{11}B DD-MAS spectra (Fig. S2 in the ESI†). In addition, powder XRD measurements indicated zigzag stacking of the boronate ester polymers (Fig. S3 in the ESI†). The stability of the microparticles was assessed by thermogravimetric analysis (TGA). No mass loss was observed up to 483 °C (Fig. S4 in the ESI†), indicating the suitability of **BP** as a polymeric support for depositing metal nanoparticles. When depositing Pd on **BP**,[23] polyethyleneimine (PEI) was employed as a binder because we reasoned that direct immobilization of the Pd would efficiently occur *via* ligand exchange.[24] The PEI-coated **BP** was characterized by zeta potential measurements, where the negative value of **BP** (−24.16 mV) was shifted to a value of +51.86 mV after being treated with PEI. Subsequently, the reduction of $PdCl_4^{2-}$ with $NaBH_4$ in a turbid solution of the as-prepared PEI-coated **BP** afforded Pd-deposited **BP** (**Pd/BP**) as a gray solid. **Pd/BP** was characterized by FE-SEM and STEM measurements, as well as atomic absorption spectroscopy. The shape and morphology of the hybrid seems to be maintained during Pd deposition (Fig. 2a). The STEM image shows that most of the Pd nanoparticles (Pd NPs) are pseudo-spherical in shape, and the interface between the Pd NPs and the boronate support material can be clearly observed (Fig. 2b). The histogram of the size distribution, being collected from 300 particles in the STEM images, suggested that highly dispersed Pd NPs (0.66 wt%) with a mean diameter of 1.52 nm and a standard deviation of 0.44 nm were loaded on the surface (Fig. 2c). Note that cluster-sized palladium was dispersed on the boronate surface. The HR-TEM image allowed us to confirm the Pd deposition on the surface; the space fringes of the Pd were

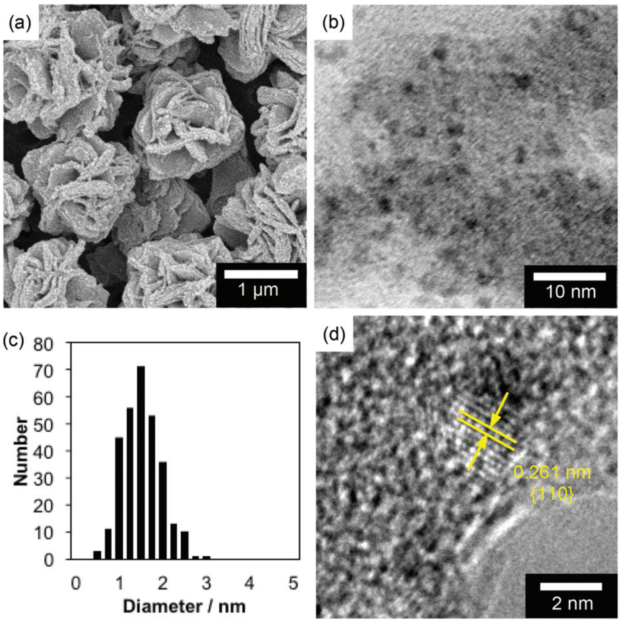

Fig. 2 (a) FE-SEM and (b) STEM images of **Pd/BP**. (c) Size distribution of Pd NPs on the **BP** support material in the STEM images. (d) HR-TEM of **Pd/BP**.

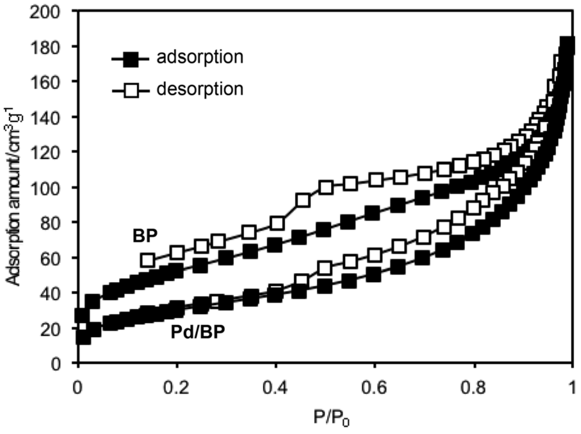

Fig. 3 N_2 adsorption–desorption isotherms of **BP** and **Pd/BP**.

determined from the image to be d = 0.261 nm (Fig. 2d), approximately consistent with the {110} facet of Pd. The EDX spectrum, furthermore, showed signals at 2.83 and 21.18 keV, which were assigned to PdLα and PdKα, respectively (Fig. S5 in the ESI†). The confirmation of the presence of metallic palladium as a major component came from the XPS measurement which showed signals at 335.16 and 340.46 eV corresponding to Pd(0) $3d_{5/2}$ and Pd(0) $3d_{3/2}$, respectively (Fig. S6 in the ESI†). The textural properties of **BP** and **Pd/BP** were estimated by N_2 adsorption–desorption measurements. According to the IUPAC classification, typical type IV isotherms with H3 hysteresis loops were observed for both **BP** and **Pd/BP** (Fig. 3), which suggests the formation of multi-layers of component polymers with a slit-type pore structure. The Brunauer–Emmett–Teller (BET) surface area (S_{BET}) of **Pd/BP** was calculated to be 107 m^2 g^{-1}, which is lower than that (184 m^2 g^{-1}) of the support material (**BP**).

Hydrogenation of CA over boronate-supported metal nanoparticles

The prepared boronate-supported metal nanoparticles were tested in the hydrogenation reaction of **CA** (Scheme 1), which was carried out in a stainless steel autoclave. Fig. 4a shows the time-dependence of the hydrogenation over the **BP**-supported Pd catalyst (**Pd/BP**) in water, as monitored by gas chromatography (GC). The reaction proceeded significantly under ambient conditions (0.1 MPa of H_2, 25 °C). For 6 h, the hydrogenation over the hybrid catalyst afforded **HCA** in 94% yield with a reaction conversion of 100%. The by-product, **PPL** (from the reduction of C=C and C=O bonds) was formed in only 6% with no detectable amount of **CAL** (product of the C=O reduction). Taking into account the low solubility of H_2 in water,[25] **Pd/BP** showed a significant catalytic activity for hydrogenation to **HCA**. When MeOH was employed as the reaction solvent (Fig. 4b),[26] a more efficient catalytic activity could be obtained; the reaction was complete within 4 h to afford **HCA** in 92% yield with a TOF value of 50 h^{-1}. It is noteworthy that further reduction to **PPL** from **HCA** was not observed under these conditions, meaning that **Pd/BP** is a selective catalyst for **HCA** *via* hydrogenation of **CA** using a green process.

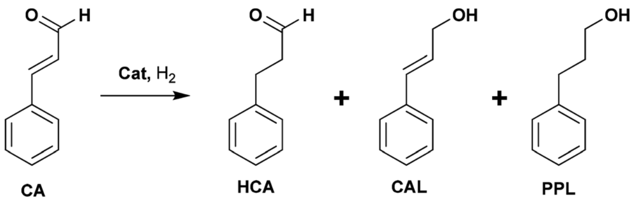

Scheme 1 Hydrogenation of cinnamaldehyde (**CA**).

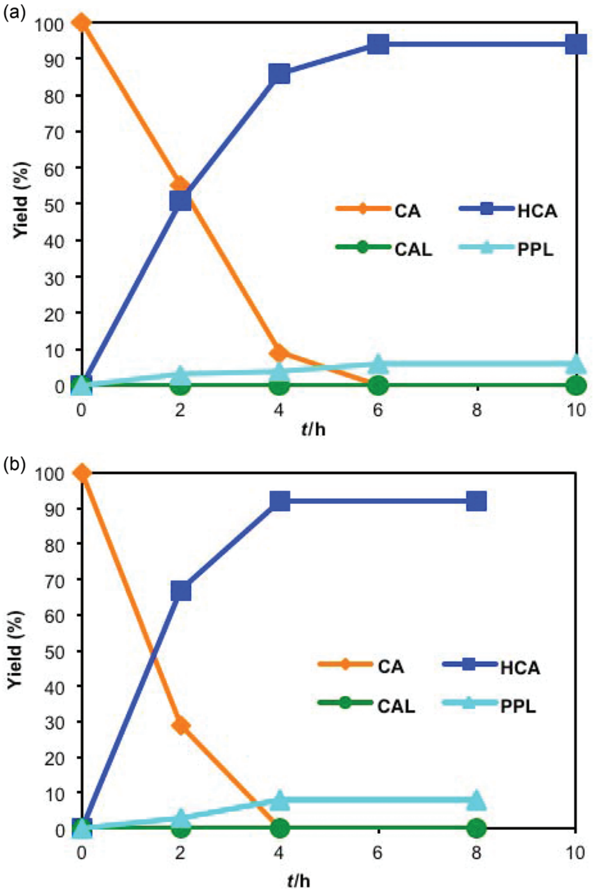

Fig. 4 Hydrogenation of **CA** (0.3 mmol) in H_2O (a) and MeOH (b) at 25 °C and 0.1 MPa in the presence of **Pd/BP** (Pd; 0.5 mol%).

Our interest is to understand what role the **BP** support plays in the catalytic activity. We thus prepared **Pd/SiO$_2$** catalysts in a similar manner, where a MeOH solution of $PdCl_4^{2-}$ in the presence of PEI-coated SiO_2 was treated with $NaBH_4$. The resulting **Pd/SiO$_2$** hybrids were characterized by HAADF-STEM, EDX, and atomic adsorption microscopy (see Fig. S7 in the ESI†); EDX Pd-mapping indicated the presence of well-dispersed Pd NPs (1.40 wt%) on the surface, with the average diameter being 1.55 ± 0.31 nm (Fig. S6b in the ESI†). To our delight, the size of the Pd NPs is consistent with the size of the Pd NPs in **Pd/BP**, allowing us to conduct a control hydrogenation using **Pd/SiO$_2$** as a catalyst. The hydrogenation in water for 4 h under similar conditions (0.1 MPa H_2, 25 °C) showed a low reactivity (TOF = 12 h^{-1}) with a reaction conversion

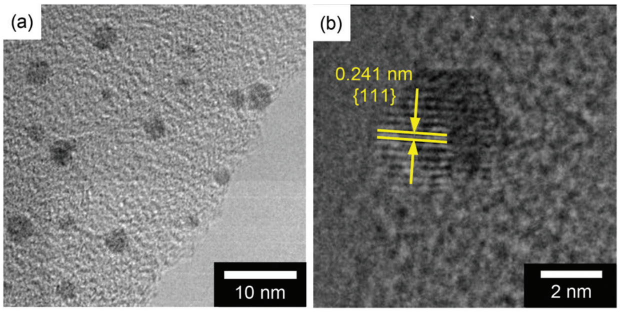

Fig. 5 (a) TEM image of **Au/BP**. (b) HR-TEM image of a lattice structure observed for the {111} facet of the Au NPs.

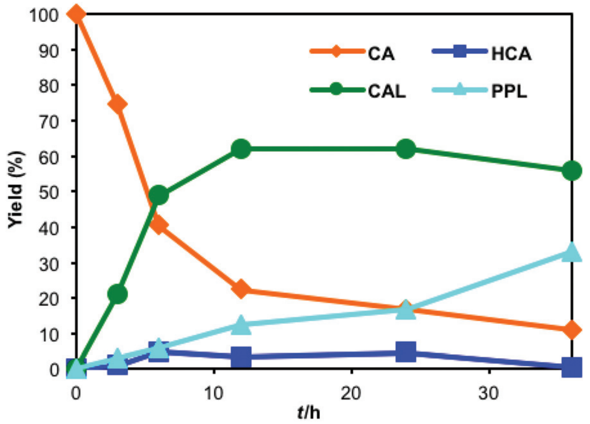

Fig. 6 Amount of **CA**, **HCA**, **CAL**, and **PPL** as a function of time in the hydrogenation of **CA** over **Au/BP** (Au; 1.1 mol%) in H_2O at 0.8 MPa H_2 and 80 °C.

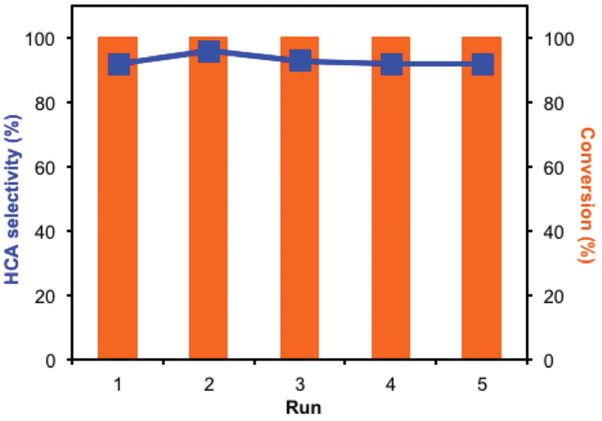

Fig. 7 Catalytic reusability of **Pd/BP** for the hydrogenation in MeOH.

of 23%, despite a significant **HCA** selectivity (87%). This means that the use of **BP** as a support material is favorable for obtaining a Pd catalyst with enhanced catalytic activity. The surface area of the **Pd/SiO$_2$** catalyst was estimated to be 571 m^2 g^{-1} (Fig. S8 in the ESI†), which is larger than that of **Pd/BP**. Therefore, the enhanced reactivity of **Pd/BP** cannot be interpreted on the basis of its surface area. It is known that catalytic activity is strongly dependent on the atomic structure of nano-palladium.[27] Further research in this regard is currently underway.

In the next stage, we examined the selective hydrogenation of **CA** to **CAL** over **Au/BP**, where Au NPs (Fig. 5) were deposited on the surface of **BP** with an average diameter of 2.7 ± 0.7 nm (Fig. S9 in the ESI†). In terms of its catalytic activity, the hydrogenation of **CA** (0.3 mmol) under 0.1 MPa H_2 at 25 °C over **Au/BP** (Au: 1.1 mol%) in water (3 mL) hardly proceeded; the reaction conversion was 5.1% after 36 h. This can be interpreted on the basis of a poor activity for dihydrogen dissociation compared to the Pd catalysts.[28] After some optimization of the reaction conditions, 0.8 MPa of H_2 at 80 °C in water allowed the hydrogenation to proceed significantly, with the conversion ratio being 78% over 12 h. Although the catalytic activity for the hydrogenation was lower than that of **Pd/BP**, 80% chemoselectivity for **CAL** was obtained, which is higher than that of ionic polymer-supported Au NP catalysts[18d] and almost similar to Au/Al_2O_3 at 4 MPa.[18a] On the other hand, when MeOH was used as a solvent **Au/BP** gave a reaction conversion of 37% with 91% chemoselectivity for **CAL** over 12 h under similar conditions. Accordingly, favorable reactivity over **Au/BP** in water (Fig. 6) may be attributed to a hydrophobic active site of **Au/BP**. It is known that the existence of Au NPs on the surface of support materials is an important factor to produce Au–H as a reducing agent,[29] leading to favorable participation in the C═O hydrogenation. Thus, the deposition of gold clusters, the diameter being less than or equal to 1.7 nm, is highly desired to improve the catalytic activity of Au-deposited **BP** towards hydrogenation.[30]

Reusability

As described above, **Pd/BP** shows good catalytic activity for the hydrogenation under mild conditions in MeOH. Accordingly, it is valuable to gain insight into its properties as a practical heterogeneous catalyst. With this in mind, we investigated the stability and reusability of **Pd/BP** in the hydrogenation using MeOH.[31] As a first run, a MeOH solution of **CA** over **Pd/BP** was stirred under 0.1 MPa of H_2 at 25 °C for 4 h. After evaluating the reaction results using GC, the catalyst was collected, washed with MeOH, and then used again in the next reaction. As shown in Fig. 7, the catalytic activity was maintained with high selectivity to HCA (>90%) over all the reaction runs, which indicates an excellent recyclability. In order to examine the shape and morphology of the **Pd/BP** catalyst after five reaction runs, FE-SEM and TEM measurements were carried out, and it seemed that the catalyst was not subject to serious damage during the reactions (Fig. S10 in the ESI†). The average diameter of the Pd NPs was estimated to be 1.94 ± 0.62 nm, somewhat larger than the Pd NPs of the as-prepared **Pd/BP** (Fig. 8). This result indicates that some aggregation of the embedded Pd occurred during the recycled reactions. However, irrespective of the cycle, the catalyst was invariably active. The amount of loaded Pd on the surface is 0.65 wt% after five successive runs, which indicates no leaching during the recycle reactions. In this way, **Pd/BP** could be reused at

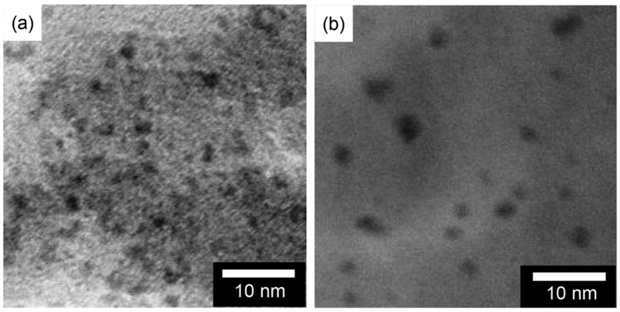

Fig. 8 (a) TEM images of as-prepared **Pd/BP** and (b) **Pd/BP** after successive five reaction runs.

least four times without appreciable loss of its catalytic activity or selectivity.

Conclusion

Hierarchical self-assembly using sequential boronate esterification led to the formation of dispersible microparticles (**BP**). Our effort to investigate **BP** as a support material led to the fabrication of nano-palladium and nano-gold catalysts for the selective hydrogenation of **CA**, a common target reaction in fine chemical synthesis. It is worth emphasizing that the Pd-deposited **BP** (**Pd/BP**) shows efficient and reusable catalytic activity with a high selectivity for **HCA** under ambient conditions in environmentally preferable solvents. Therefore, the practical use of **Pd/BP** as a heterogeneous catalyst in the sustainable production of fine chemicals merits further investigation.

Acknowledgements

This research was supported by a Grant-in-Aid for Scientific Research from the Ministry of Education, Science, Sports and Culture of Japan (no. 24350075). We thank Dr A. Taketoshi (Haruta Laboratory) of Tokyo Metropolitan University for her kind support in this study.

Notes and references

1 (*a*) F. J. M. Hoeben, P. Jonkheijm, E. W. Meijer and A. P. H. J. Schenning, *Chem. Rev.*, 2005, **105**, 1491; (*b*) F. Cheng and F. Jäkle, *Polym. Chem.*, 2011, **2**, 2122; (*c*) C. Park, J. Lee and C. Kim, *Chem. Commun.*, 2011, **47**, 12042; (*d*) L. Maggini and D. Bonifazi, *Chem. Soc. Rev.*, 2012, **41**, 211; (*e*) L. Wang, L. Xu, H. Kuang, C. Xu and N. A. Kotov, *Acc. Chem. Res.*, 2012, **45**, 1916; (*f*) S.-L. Li, T. Xiao, C. Lin and L. Wang, *Chem. Soc. Rev.*, 2012, **41**, 5950; (*g*) C. Li and S. Liu, *Chem. Commun.*, 2012, **48**, 3262.

2 R. Umeda, H. Awaji, T. Nakahodo and H. Fujihara, *J. Am. Chem. Soc.*, 2008, **130**, 3240.

3 P. Zhang, Z. Weng, J. Guo and C. Wang, *Chem. Mater.*, 2011, **23**, 5243.

4 (*a*) J. Xu, G. Chen, R. Yan, D. Wang, M. Zhang, W. Zhang and P. Sun, *Macromolecules*, 2011, **44**, 3730; (*b*) Y. M. A. Yamada, S. M. Sarkar and Y. Uozumi, *J. Am. Chem. Soc.*, 2012, **134**, 3190.

5 (*a*) Y. Huang, H. Ma, S. Wang, M. Shen, R. Guo, X. Cao, M. Zhu and X. Shi, *ACS Appl. Mater. Interfaces*, 2012, **4**, 3054; (*b*) M. A. Khalily, O. Ustahuseyin, R. Garifullin, R. Genc and M. O. Guler, *Chem. Commun.*, 2012, **48**, 11358.

6 B. Yuan, Y. Pan, Y. Li, B. Yin and H. Jiang, *Angew. Chem., Int. Ed.*, 2010, **49**, 4054.

7 S.-Y. Ding, J. Gao, Q. Wang, Y. Zhang, W.-G. Song, C.-Y. Su and W. Wang, *J. Am. Chem. Soc.*, 2011, **133**, 19816.

8 (*a*) T. D. James, P. Linnane and S. Shinkai, *Chem. Commun.*, 1996, 281; (*b*) H. Höpfl, *Struct. Bonding*, 2002, **103**, 1; (*c*) N. Fujita, S. Shinkai and T. D. James, *Chem. – Asian J.*, 2008, **3**, 1076; (*d*) K. Severin, *Dalton Trans.*, 2009, 5254; (*e*) A. L. Korich and P. M. Iovine, *Dalton Trans.*, 2010, **39**, 1423; (*f*) R. Nishiyabu, Y. Kubo, T. D. James and J. S. Fossey, *Chem. Commun.*, 2011, **47**, 1124; (*g*) X. Wu, Z. Li, X.-X. Chen, J. S. Fossey, T. D. James and Y.-B. Jiang, *Chem. Soc. Rev.*, 2013, **42**, 8032.

9 R. Nishiyabu, S. Teraoka, Y. Matsushima and Y. Kubo, *ChemPlusChem*, 2012, **77**, 201.

10 Y. Matsushima, R. Nishiyabu, N. Takanashi, M. Haruta, H. Kimura and Y. Kubo, *J. Mater. Chem.*, 2012, **22**, 24124.

11 R. Nishiyabu, Y. Sugino and Y. Kubo, *Chem. Commun.*, 2013, **49**, 9869.

12 S. Minakata and M. Komatsu, *Chem. Rev.*, 2009, **109**, 711.

13 C. Capello, U. Fischer and K. Hungerbühler, *Green Chem.*, 2007, **9**, 927.

14 (*a*) M. Boudart, *Nature*, 1994, **372**, 320; (*b*) S. Schimpf, J. Gaube and P. Claus, Selective hydrogenation of multiple unsaturated compounds, in *Springer Series in Chemical Physics*, 2004, vol. 75, p. 85.

15 (*a*) S. Mahmoud, A. Hammoudeh, S. Gharaibeh and J. Melsheimer, *J. Mol. Catal. A: Chem.*, 2002, **178**, 161; (*b*) P. Mäki-Arvera, J. Hájek, T. Salmi and D. Y. Murzin, *Appl. Catal., A*, 2005, **292**, 1.

16 P. Gallezot and D. Richard, *Catal. Rev. Sci. Eng.*, 1998, **40**, 81.

17 Selective hydrogenation to **HCA** over heterogeneous catalysts; for example, see: (*a*) F. Benvenuti, C. Carlini, M. Marchionna, A. M. R. Galletti and G. Sbrana, *J. Mol. Catal. A: Chem.*, 1999, **145**, 221; (*b*) J.-P. Tessonnier, L. Pesant, G. Ehret, M. J. Ledoux and C. Pham-Huu, *Appl. Catal., A*, 2005, **288**, 203; (*c*) Y. Kume, K. Qiao, D. Tomida and C. Yokoyama, *Catal. Commun.*, 2008, **9**, 369; (*d*) S. Bhogeswararao and D. Srinivas, *Catal. Lett.*, 2010, **140**, 55; (*e*) A. M. R. Galletti, C. Antonetti, A. M. Venezia and G. Giambastiani, *Appl. Catal., A*, 2010, **386**, 124; (*f*) K. Strzelec, K. Wasikowska, M. Cypryk and P. Pospiech, *e-Polymers*, 2011, **024**, 1; (*g*) C. Stangel, G. Charalambidis, V. Varda, A. G. Coutsolelos and I. D. Kostas, *Eur. J. Inorg. Chem.*, 2011, 4709; (*h*) A. Ungureanu, B. Dragoi, A. Chirieac,

S. Royer, D. Duprez and E. Dumitriu, *J. Mater. Chem.*, 2011, **21**, 12529; (*i*) Z.-C. Zhang, X. Zhang, Q.-Y. Yu, Z.-C. Liu, C.-M. Xu, J.-S. Gao, J. Zhuang and X. Wang, *Chem. – Eur. J.*, 2012, **18**, 2639; (*j*) A. M. R. Galletti, L. Toniolo, C. Antonetti, C. Evangelisti and C. Forte, *Appl. Catal., A*, 2012, **447–448**, 49; (*k*) S. Bhogeswararao, V. P. Kumar, K. V. R. Chary and D. Srinivas, *Catal. Lett.*, 2013, **143**, 1266; (*l*) A.-M. Simion, T. Arimura and C. Simion, *C. R. Chim.*, 2013, **16**, 476; (*m*) N. Mingming, W. Yanhua, L. Wenjiang, J. Jingyang and J. Zilin, *Chin. J. Catal.*, 2013, **34**, 674.

18 Selective hydrogenation to **CAL** over heterogeneous catalysts; for example, see: (*a*) E. Bus, R. Prins and J. A. van Bokhoven, *Catal. Commun.*, 2007, **8**, 1397; (*b*) E. V. Ramos-Fernández, J. Ruiz-Martínez, J. C. Serrano-Ruiz, J. Silvestre-Albero, A. Sepúlveda-Escribano and F. Rodríguez-Reinoso, *Appl. Catal., A*, 2011, **402**, 50; (*c*) M.-M. Wang, L. He, Y.-M. Liu, Y. Cao, H.-Y. He and K.-N. Fan, *Green Chem.*, 2011, **13**, 602; (*d*) I. Biondi, G. Laurenczy and P. J. Dyson, *Inorg. Chem.*, 2011, **50**, 8038; (*e*) K. J. A. Raj, M. G. Prakash, T. Elangovan and B. Viswanathan, *Catal. Lett.*, 2012, **142**, 87; (*f*) Y. Zhang, X. Cui, F. Shi and Y. Deng, *Chem. Rev.*, 2012, **112**, 2467; (*g*) M. Stratakis and H. Garcia, *Chem. Rev.*, 2012, **112**, 4469; (*h*) F. Cárdenas-Lizana and M. A. Keane, *J. Mater. Sci.*, 2013, **48**, 543; (*i*) T. Mitsudome and K. Kaneda, *Green Chem.*, 2013, **15**, 2636.

19 (*a*) H. Hagiwara, T. Nakamura, T. Hoshi and T. Suzuki, *Green Chem.*, 2011, **13**, 1133; (*b*) R. Nakao, H. Rhee and Y. Uozumi, *Org. Lett.*, 2005, **7**, 163; (*c*) N. M. Callis, E. Thiery, J. L. Bras and J. Muzart, *Tetrahedron Lett.*, 2007, **48**, 8128.

20 S. C. Mhadgut, K. Palaniappan, M. Thimmaiah, S. A. Hackney, B. Török and J. Liu, *Chem. Commun.*, 2005, 3207.

21 M.-M. Wang, L. He, Y.-M. Liu, Y. Cao, H.-Y. He and K.-N. Fan, *Green Chem.*, 2011, **13**, 602.

22 The concentration was based on the monomer unit.

23 The amount of loaded Pd on the surface of PEI-free **BP** was 0.09% after reduction of $PdCl_4^{2-}$ with $NaBH_4$.

24 X. Zhou, W. Xu, Y. Wang, Q. Kuang, Y. Shi, L. Zhong and Q. Zhang, *J. Phys. Chem. C*, 2010, **114**, 19607.

25 C. L. Young, *Hydrogen and Deuterium, Pergamon, Solubility data series*, 1981, vol. 5/6.

26 The mole fraction solubility for H_2 in MeOH has been reported to be 1.61×10^{-4} (25 °C),[25] being higher than that in water.

27 M. Shao, T. Yu, J. H. Odell, M. Jin and Y. Xia, *Chem. Commun.*, 2011, **47**, 6566.

28 M. Haruta, *Faraday Discuss.*, 2011, **152**, 11.

29 (*a*) T. Ishida, N. Kawakita, T. Akita and M. Haruta, *Gold Bull.*, 2009, **42**, 267; (*b*) R. Juárez, S. F. Parker, P. Concepción, A. Corma and H. García, *Chem. Sci.*, 2010, **1**, 731.

30 A. Viskovskiy, H. Matsumoto, K. Mitsuhara, T. Nakada, T. Akita and Y. Kido, *Phys. Rev. B: Condens. Matter Mater. Phys.*, 2011, **83**, 165428.

31 A low recyclability of the **Au**/**BP** catalyst was observed for the hydrogenation under 0.8 MPa of H_2 at 80 °C in water for 12 h. After one cycle, the hydrogenation of **CA** over **Au**/**BP** under the same conditions afforded **CAL** in 52% selectivity with a 29% reaction conversion. The low stability of the catalyst is due to mechanical damage from the reactor, which serves to aggregate the Au NPs, with the size distribution being 5.8 ± 3.4 nm.